Available online at www.sciencedirect.com
SCIENCE DIRECT®
Carbohydrate Research 340 (2005) 791–809
Carbohydrate RESEARCH

Perspective

Experimental approaches to hyaluronan structure

Mary K. Cowman[a,*] and Shiro Matsuoka[b]

[a]*Othmer Department of Chemical and Biological Sciences and Engineering, Polytechnic University, 6 Metrotech Center, Brooklyn, NY 11201, USA*
[b]*Department of Biomedical Engineering, Columbia University, 503 West 120th Street, MC8904, New York, NY 10027, USA*

Received 16 October 2004; accepted 10 January 2005

Dedicated to Professor David A. Brant, in honor of his pioneering work on carbohydrate conformation

Abstract—A review of the literature describing experimental studies on hyaluronan (HA) is presented. Methods sensitive to the hydrodynamic properties of HA, analyzed in neutral aqueous solution containing NaCl at physiological concentration, can be shown to fit the expected behavior of a high molecular weight linear semi-flexible polymer. The significant nonideality of HA solutions can be predicted by a simple treatment for hydrodynamic interactions between polymer chains. Nuclear magnetic resonance and circular dichroism studies of HA are also in agreement with a model incorporating dynamically formed and broken hydrogen bonds, contributing to the semi-flexibility of the polymer chain, and segmental motions on the nanosecond time scale.

HA shows the capability for self-association in the formation of a viscoelastic putty state at pH 2.5 in the presence of salt, and a gel state at pH 2.5 in mixed organic/aqueous solution containing salt. Ordered and associated structures have also been observed for HA on the surfaces, especially in the presence of surface-structured water. These phenomena can be understood in terms of counterion-mediated polyelectrolyte interactions. The possibility that hyaluronan exists in vivo in environments that induce ordered structures and assemblies is discussed.

Keywords: Hyaluronan; Polysaccharide; Viscosity; Polymer solution; Osmotic pressure; Atomic force microscopy

1. Introduction

Hyaluronan (HA) is a high molecular weight linear polysaccharide, with the structure poly[(1→3)-2-acetamido-2-deoxy-β-D-glucopyranosyl-(1→4)-β-D-glucopyranosyluronic acid]. It has one carboxylate group per disaccharide repeat, and is therefore a polyelectrolyte. There are no known deviations from the linear repeating disaccharide structure, with the possible exception of occasional deacetylated glucosamine residues. The molecular weight of HA can range as high as 6000–8000 kDa, in synovial fluid, eye vitreous, and rooster comb.[1] A stretched chain of HA with a molecular weight of 6000 kDa would have an approximate length of 15 μm, and a diameter of about 0.5 nm. Isolation of HA from normal skin, muscle, heart, lung, small intestine, large intestine, etc., frequently yields a lower molecular weight polymer, but this is probably the result of degradation during isolation, since recent data for HA isolated from those tissues in the presence of desferoxamine shows only high molecular weight.[2] HA can be chemically degraded by hydroxyl radicals and peroxynitrite,[3] which may be generated in inflammatory conditions or during tissue remodeling. For example, reduced molecular weight HA has been observed in osteoarthritis.[4,5]

HA is found primarily in the extracellular matrix and pericellular matrix, but has also been shown to occur intracellularly. The biological functions of HA include maintenance of the elastoviscosity of liquid connective tissues such as joint synovial fluid and eye vitreous, control of tissue hydration and water transport, supramolecular assembly of proteoglycans in the extracellular matrix, and numerous receptor-mediated roles in cell

* Corresponding author. Tel.: +1 718 260 3054; fax: +1 718 260 3125; e-mail: mcowman@poly.edu

0008-6215/$ - see front matter © 2005 Elsevier Ltd. All rights reserved.
doi:10.1016/j.carres.2005.01.022

detachment, mitosis, migration, tumor development and metastasis, and inflammation.[6–13]

In the extracellular matrix, under normal physiological conditions, HA is generally believed to exist as crowded random coil molecules. The structure of HA under specific pathological conditions can be quite different. In smooth muscle cells exposed to viral mimics or agents causing endoplasmic reticulum stress, HA is produced in the form of huge cable-like assemblies linking cells together, and having specific binding interactions with unactivated mononuclear leukocytes, thus mediating the inflammatory response.[13–15]

The extensive repertoire of biological functions of HA suggests the existence of a correspondingly large repertoire of HA conformations and specific binding interactions. It is likely that the conformation is affected by the local environment, including ionic strength and specific ion interactions, local dielectric constant, excluded volume effects, tethering to surfaces and fixed macromolecular assemblies, exposure to perturbing mechanical forces, and the presence of interacting species (including but not limited to proteins and lipids).

The goal of this perspective article on HA, which expands on two other recent reviews covering portions of the available data,[16,17] is to summarize the current state of knowledge derived from a broad (but not exhaustive) range of experimental studies on HA, incorporating recent advances in the polymer theory.

2. HA in the solid state

The conformation of HA in the solid state was determined by X-ray diffraction of stretched fibers.[18–21] Single helical conformations containing 2, 3, or 4 disaccharides per helical turn were found, depending on the counterion present (H^+, Na^+, K^+, Ca^{2+}, etc.). All of these structures look rather like stretched coiled telephone cords. A double helix, containing four disaccharides per turn, was also observed[22,23] under unusual ionic conditions (mixed H^+/K^+, Rb^+, NH_4^+). All of these structures are stabilized by hydrogen bonds linking adjacent sugar residues across both glycosidic linkages.

3. Experiments sensitive to the global conformation of HA in solution

HA in neutral aqueous solution, at or near a physiological concentration of NaCl, generally behaves as a typical semi-flexible polymer molecule. Short chains are somewhat extended, while longer chains show evident coiling. The molecular domain of a high molecular weight HA chain occupies a sphere, as the time average of all accessible conformations. Because the molecular domains are quite large (but not impenetrable), HA chains interfere with each other at even low concentrations. This intermolecular interaction leads to large nonideality contributions to the experimental data, which have sometimes been interpreted as evidence for the existence of stable networks. This is shown to be incorrect for HA in physiological saline solutions. Certain other conditions have been found to enhance intermolecular interaction, as detailed below.

4. Theoretical framework for data interpretation: rheology

One of the most noticeable characteristics of HA solutions is high viscosity. The viscous properties of HA have therefore been studied quite extensively. These studies generally seek to determine the effect of variables such as concentration, molecular weight, temperature, ionic strength, shear rate, etc., on the solution viscosity. They also seek to use this information to identify the molecular domain shape, expansion, rigidity, and possible intermolecular interactions. Deviations in behavior from theoretical predictions may provide insight into formation of aggregates or other self-associated species. Sometimes these studies are performed on HA samples of narrow polydispersity, but often the samples have broad unknown molecular weight distributions.

A detailed discussion of the origins and uses of the relevant equations for analysis of HA solution viscosity is beyond the scope of this literature review, and is given elsewhere.[24–28] Briefly, we may state that the specific viscosity, η_{sp}, measured for homogeneous 'well-behaved' HA solutions at very low or zero shear rate is a simple function of the concentration, c, and average molecular weight of the HA, described in terms of its intrinsic viscosity $[\eta]$:

$$\eta_{sp} = c[\eta] + k'(c[\eta])^2 + \frac{(k')^2}{2!}(c[\eta])^3 + \frac{(k')^3}{3!}(c[\eta])^4 \quad (1)$$

where the value of k', the Huggins constant, is explicitly 0.4, based on its derivation from the Stokes–Einstein equation for the viscosity of a suspension of spheres. A plot of the equation and its component terms is given in Figure 1. This four-term interaction equation is analogous to a virial expansion in which the (usually repulsive) interactions between molecules at finite concentrations increase the solution viscosity greatly over the extremely dilute solution case. The first term of Eq. 1, $c[\eta]$, is the limiting value of the specific viscosity at infinite dilution. The entire right side of the equation is $c[\eta]$ multiplied by a nonideality factor, $\exp(k'c[\eta])$, expressed as the expansion $(1 + k'c[\eta] + (k'c[\eta])^2/2! + (k'c[\eta])^3/3! + \cdots)$, truncated to include only the first four terms. The term $k'c[\eta]$ is equal to the volume fraction, ϕ, of polymer in dilute solution if $k' = 0.4$. This follows from the Stokes–Einstein equation for the viscosity of a suspension of spheres, given as $\eta_{sp} = 2.5\phi$, from which $\phi = 0.4\eta_{sp} = 0.4c[\eta]$ at infinite dilution. The term $k'c[\eta]$ is therefore a measure of the degree to which

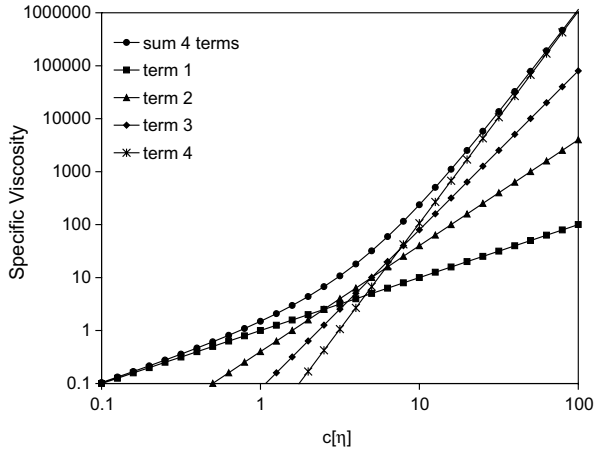

Figure 1. Dependence of the specific viscosity on interactions between macromolecules, as expressed by the four-term equation (Eq. 1). Each term depends on the coil overlap factor to a different power.

the domains of the polymer coils overlap in dilute or semi-dilute solution. Eq. 1 is not derived with any consideration to the entanglement concept, and indeed is applicable for even rigid polymers, for which the entanglement concept is not meaningful. The hydrodynamic interaction model for viscosity data fitting and interpretation applies to HA and many other polymers in solution, because these solutions are not truly concentrated solutions, and far from the melt condition for which the entanglement concept was developed. For example, the highest concentration at which HA has been studied is about 8% by weight. Considering the partial specific volume of HA to be about 0.56 cm^3/g, the volume fraction of HA in that case would be about 4.5%. The solution is still more than 95% water, and hydrodynamic interactions continue to dominate the viscous properties.

It should be noted that HA solutions containing undissolved aggregate or other nonequilibrium structures are not 'well-behaved', and may yield data that cannot be fit by the above equation. In fact, failure to follow the expected relationship may suggest the presence of such anomalies.

The above equation requires that the specific viscosity and the intrinsic viscosity be measured under the same set of conditions. For example, the most commonly used conditions for the study of HA include the use of sufficient ionic strength (generally $\geqslant 0.1$ M) to mask electrostatic repulsions, using NaCl as supporting electrolyte, at neutral pH, and at a temperature of approximately 20–37 °C. For such conditions, the relationship between the intrinsic viscosity and average molecular weight, M, of the HA has already been established, and the intrinsic viscosity may be calculated from the molecular weight, if determined by an alternative technique. These relationships follow the form of the Mark–Houwink–Sakurada equation, $[\eta] = KM^a$, where K and a are constants for a given set of conditions, and for a given range of molecular weight.

The intrinsic viscosity is a measure of the hydrodynamic volume of the HA chain in solution. It is equal to 2.5 times the specific volume, V_s, which has units of volume per unit mass, usually expressed as mL/g. It is also equal to 2.5 (V_m/M), where V_m is the molar volume. The molar volume can be used to estimate the hydrodynamic diameter of a molecule, when an approximately spherical model is appropriate for the expanded chain domain in solution.

Where it is of interest to determine the intrinsic viscosity, for example, as a way to determine the HA molecular weight, this may be done by low shear capillary viscometry or rheometer capable of low shear measurement. The conventional procedure is to measure the viscosity of solutions that are sufficiently dilute that only the first two terms of Eq. 1 are required. This is the Huggins equation, and the usual procedure involves plotting η_{sp}/c versus c, to obtain a straight line with $[\eta]$ as the y-intercept and the Huggins constant from the slope, $k'[\eta]^2$. What constitutes a sufficiently dilute solution depends on the molecular weight. In general, it is necessary to use solutions for which the product of the concentration and intrinsic viscosity does not exceed 1. For example, HA of 3×10^6 average molecular weight would have an intrinsic viscosity (at zero shear) of about 4400 mL/g, and should be analyzed in solutions below about 2.3×10^{-4} g/mL (230 μg/mL). Failure to follow this restriction often leads to erroneously high values of the Huggins constant and low values of the intrinsic viscosity. If it is necessary or desirable to use higher concentrations, then the higher order terms of Eq. 1 must be added. As stated above, the four-term equation may be recognized as a truncated form of the exponential equation derived by Martin:

$$\eta_{sp} = c[\eta] \exp(k'c[\eta]) \tag{2}$$

An alternative form of this equation, namely the logarithmic form,

$$\ln\left(\frac{\eta_{sp}}{c}\right) = \ln[\eta] + k'[\eta]c \tag{3}$$

provides a linear plot of $\ln(\eta_{sp}/c)$ versus c that is valid up to about $c[\eta] = 3.5$.

Having measured the intrinsic viscosity, one may use it to estimate such molecular parameters as the time-average and ensemble-average hydrodynamic volume of the HA, or the persistence length of the chain, both being measures of the apparent stiffness of the chain and its consequent expansion.

The shear rate dependence of the viscosity of HA solutions provides additional information about the hydrodynamic volume. When the shear rate exceeds the rate at which HA chains can relax, the chains remain distorted and the viscosity drops. The critical shear rate

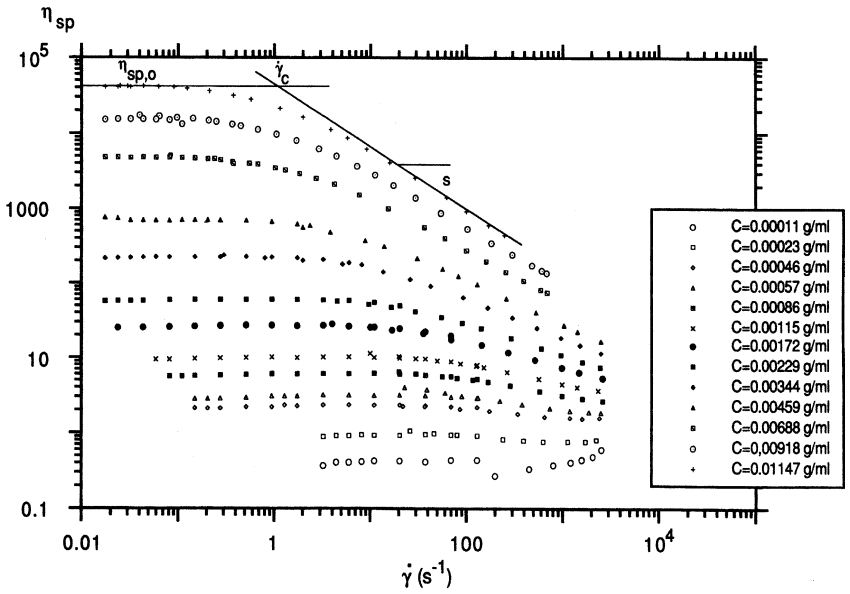

Figure 2. Shear thinning of solutions containing HA with a molecular weight of 2.2×10^6 in 0.1 M NaCl at 25 °C. The critical shear rate depends on the relaxation time of the hyaluronan polymer. Reprinted with permission from Fouissac, E.; Milas, M.; Rinaudo, M. *Macromolecules* **1993**, *26*, 6945–6951. Copyright 1993 American Chemical Society.

is related to the inverse relaxation time (Fig. 2). The relaxation time depends on the molecular volume. In infinitely dilute solution, the longest relaxation time, τ_0, is proportional to the solvent viscosity, η_0, and the molar hydrodynamic volume, V_m:

$$\tau_0 \propto \frac{\eta_0}{RT} V_m \propto \frac{\eta_0}{RT} [\eta] M \tag{4}$$

where R is the gas constant, and T is the temperature. For HA, the intrinsic viscosity is proportional to the molecular weight raised to the 0.8 power, so both the molar hydrodynamic volume and τ_0 are proportional to the molecular weight raised to the 1.8 power.

With increasing concentration or molecular weight, the polymer chains begin to approach each other and interact hydrodynamically. By analogy to the treatment of the effective specific volume of the polymer coil, we can consider the hydrodynamic interactions to increase the effective molar volume of the polymer. The form of the dependence is again based on the volume fraction, or coil overlap parameter, as a weighting factor, which determines the relative likelihood of intermolecular interactions. If we allow for intermolecular interaction of a given polymer with an infinite number of neighbors, the relaxation time, τ, at a given concentration and molecular weight is

$$\tau \propto \frac{\eta_0}{RT} [\eta] M \exp(k' c [\eta]) \tag{5}$$

This is analogous to the Martin equation for the viscosity. Patel and Takahashi[29] have shown that such an equation is appropriate for the relaxation time measured by dielectric relaxation spectroscopy for polyisoprene in hydrocarbon solvent. For viscosity data, the Martin equation overestimates the intermolecular effects. Thus for HA and many other polymers, experimental viscosity data had indicated the need to consider interactions with no more than about three neighbors simultaneously, and we found only the first four terms of the expansion of the exponential to be necessary to fit the data. Similarly, available experimental data for the relaxation time of HA (see below) is approximately matched by using only the first three terms. We find the relaxation time to depend on interactions of one chain with up to two neighbors, and use the following equation:

$$\tau \propto \frac{\eta_0}{RT} \left([\eta] M + k' c [\eta]^2 M + \frac{(k')^2}{2!} c^2 [\eta]^3 M \right) \tag{6}$$

The viscoelastic relaxation time may be measured in one of two ways. In shear flow measurements, the relaxation time is proportional to the inverse of the critical shear rate. In the second approach to measurement of the relaxation time, the behavior of the polymer solution under dynamic oscillatory conditions is measured. At frequencies below that corresponding to the critical shear rate above, the polymer solution behaves as a viscous solution; at higher frequencies it behaves elastically. These properties are reflected in the changes in the elastic storage modulus, G', and viscous loss modulus, G'', curves as a function of frequency (Fig. 3). The transition from viscous to elastic behavior is marked by the crossover point of the two curves. The relaxation time is proportional to the inverse of the crossover frequency.

At high frequencies of oscillatory deformation, the elastic modulus of concentrated polymer solutions reaches a plateau value. This plateau is conventionally interpreted as evidence for the existence of an entangled polymer network. Whereas the elastic modulus, G_e, for dilute solutions is proportional to c/M, the terminal elastic modulus for more concentrated solutions is considered to be independent of the molecular weight. We may predict the effect of hydrodynamic interaction on the elastic modulus by considering our expressions for the viscosity and relaxation time, and the relationship between these quantities and the modulus. For dilute solutions, we may use the first term of the four-term interaction equation for the solution specific viscosity (Eq. 1) and its counterpart for the relaxation time (Eq. 6) to determine G_e for dilute solutions.

$$G_e = \frac{\eta}{\tau} \propto \frac{c[\eta]}{[\eta]M} \propto \frac{c}{M} \tag{7}$$

For relatively more concentrated solutions, the modulus will vary as the largest term in each series; these are the fourth term of the viscosity expansion, and the third term of the relaxation time expansion. Thus G_e for semidilute solutions will vary as approximately

$$G_e \propto \frac{c^4[\eta]^4}{c^2[\eta]^3 M} \propto c^2\frac{[\eta]}{M} \propto c^2\frac{M^{0.8}}{M} \propto c^2 M^{-0.2} \tag{8}$$

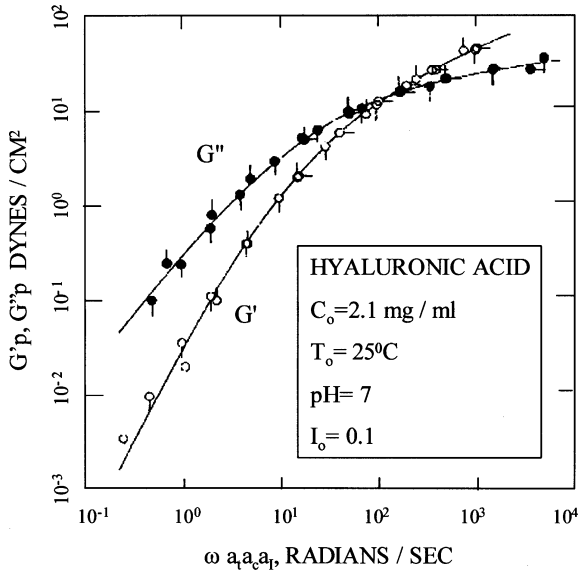

Figure 3. Master curves for the elastic modulus (G') and the viscous modulus (G'') of a solution of HA with a molecular weight of 2.8×10^6 as a function of the frequency of displacement. Reprinted with permission from Gibbs, D. A.; Merrill, E. W.; Smith, K. A.; Balazs, E. A. *Biopolymers* **1968**, *6*, 777–791. Copyright 1968 John Wiley and Sons, Inc.

5. Theoretical framework for data interpretation: other methods sensitive to global conformation

HA has been studied by a number of other physicochemical techniques that depend on the global structure of the macromolecule, as well as interactions between molecules at finite concentrations. The conventional procedure is to express the experimental data in terms of a limiting value characteristic of the isolated molecule (obtained by extrapolation to zero concentration) and concentration-dependent terms in the form of an expansion with coefficients called virial coefficients (e.g., A_2, the second virial coefficient, etc) or other scaling parameters. In a parallel approach, we previously described the application of the interaction equation to the expression for osmotic pressure, π, of polymer solutions.[25] The nonideality term is $\exp(k'c[\eta])$, or equivalently $\exp(c/c^*)$, where c^* is the critical concentration at which the expanded molecular coils fill the solution space. Again, we find that only a limited number of terms of the expansion for the exponential term are needed to fit the experimental data, since the number of simultaneous intermolecular interactions is limited in a real solution. For the osmotic pressure, we find three terms to be sufficient.

$$\frac{\pi}{cRT} = \frac{1}{M}\exp(k'c[\eta]) = \frac{1}{M} + \left(\frac{k'[\eta]}{M}\right)c + \left(\frac{(k')^2[\eta]^2}{2M}\right)c^2 \tag{9}$$

Burchard[30] additionally showed that the nonideality of the reduced osmotic modulus can be considered to take the form of an expansion of the term A_2Mc. The Burchard approach is identical to our approach, when $k'c[\eta]$ is taken equal to A_2Mc. Burchard further extended the use of this expansion to analysis of the concentration and angular dependence of light scattering data, using the nonideality term as a correction relating the real mass measured by extrapolation to zero concentration to an apparent mass measured at any given finite concentration (i.e., M/M_{app}). Equating $k'c[\eta]$ with A_2Mc indicates that A_2 should be dependent on the molecular weight to a low degree (-0.2 power for HA, for which the exponent a is 0.8):

$$A_2 = \frac{k'[\eta]}{M} = 0.4KM^{a-1} \propto M^{-0.2} \tag{10}$$

This is in agreement with Burchard's measurement of $A_2 \propto M^{-0.236}$ for linear polystyrene, a flexible polymer. Burchard provides an elegant overview of the concentration and molecular weight dependence of data from several physicochemical techniques for polysaccharides in solution, in which the data for different polysaccharides fall on discrete curves according to their molecular shapes. If the molecular weight dependence of the second virial coefficient in Eq. 10 is considered, and its

origin in the shape-sensitive intrinsic viscosity is understood, then we can expect to see a more universal expression prove to be applicable.

The application of elastic light scattering analysis to the characterization of HA has recently been reviewed.[28] Briefly, the most common methods for static light scattering analysis are WALS, wide-angle light scattering, and MALS, multi-angle light scattering. The scattering is measured as a function of HA concentration and of scattering angle. The data are usually analyzed with the Zimm plot (Fig. 4), which allows simultaneous extrapolation to zero angle and zero concentration. Light scattering provides the most accurate measure of the weight-average molecular weight of HA. The second virial coefficient is obtained from the slope of the concentration dependence of the scattering at zero angle. In addition, the radius of gyration, characterizing the molecular expansion, can be obtained from the angular dependence of the scattering extrapolated to zero concentration. The predicted dependence for the radius of gyration on the molecular weight is $R_G \propto M^{\nu}$, where ν is near 0.6 for a high molecular weight polymer, treated as a freely jointed chain in a good solvent, thus having the maximum excluded volume contribution.

In the past few years, combined size exclusion chromatography (SEC) with MALS detection has become a standard method for analysis of HA molecular weight distributions. The data analysis includes measurement of the radius of gyration and molecular weight continuously as sample elutes, providing an immediate calculation of the molecular weight distribution (Fig. 5). It should be noted that the second virial coefficient is often ignored in the default setting software for such systems, but that it should be included for most accurate work, because HA chains begin to interact at even low concentrations. A newer method is flow field–flow fractionation with MALS. Takahashi et al.[31] have established this method, and shown that the second virial coefficient of

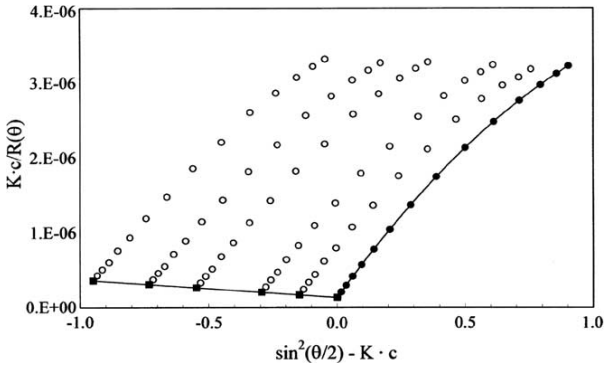

Figure 4. Zimm plot of light scattering data from HA solution in physiological saline. The hyaluronan molecular weight was 7.4×10^6 (Ref. 28).

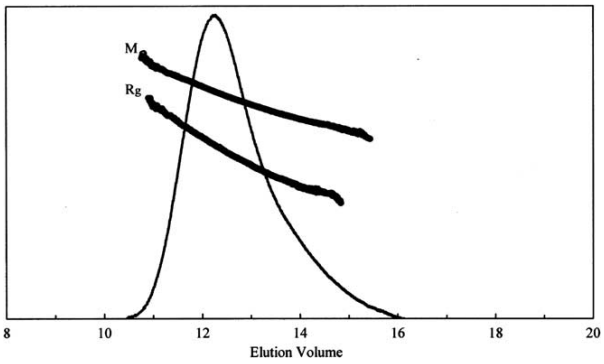

Figure 5. Size exclusion chromatography with multiangle light scattering (SEC–MALS) of HA with a molecular weight of 1.0×10^6. The molecular weight and radius of gyration are determined on-line, as a function of elution volume (Ref. 28).

$A_2 = 0.022 M_w^{-0.19}$ works well to correct the data for nonideality in concentration dependence. This is a stunning agreement with the simple expression given in Eq. 10.

Diffusion coefficients, inversely related to the effective hydrodynamic radius, also provide information on the parameters of isolated chains when data are extrapolated to zero concentration, and provide another window into the intermolecular interactions that inhibit movement as the coil overlap factor increases. Hardingham[17] has recently reviewed the use of confocal fluorescence recovery after photobleaching (confocal FRAP) as a method allowing diffusion coefficients to be measured for HA without any external perturbation of the solution, such as shear. The data analysis employs a scaling equation relating the measured self-diffusion coefficient, D, to D_0, the limiting value obtained by extrapolation to zero concentration:

$$D = D_0 \exp(-\alpha c^{\nu}) \tag{11}$$

The scaling constants α and ν are adjustable parameters, and vary with the sample. This equation is clearly similar to the Martin equations for solution specific viscosity, but a quantitative comparison has not been made.

The experimental data for HA solutions obtained by osmotic pressure, light scattering, sedimentation, and diffusion techniques can be compared with predictions for well-behaved polymer solutions. The predicted behavior accounts for nonspecific and transient intermolecular interactions, whereas significant deviations from prediction, if any, could indicate self-association under specific conditions.

6. Summary of experimental results from viscometric analyses

6.1. HA in neutral aqueous NaCl solutions

Figure 6 illustrates the dilute solution viscometric behavior of HA in 0.15 M NaCl at 25 °C. For the rela-

tionship between $\log[\eta]$ and $\log M$, the data may be approximately fit as two distinct linear regions (although the wormlike chain model more accurately explains the smooth transition; see below). This phenomenon was first reported by Cleland and co-workers[32,33] and subsequently Shimada and Matsumura.[34] In the low molecular weight region, corresponding to the free-draining chain conformation, the slope is approximately 1.16. In the high molecular weight region, corresponding to the nonfree-draining ball-like conformation, the slope is approximately 0.80. These values lead to an estimation of the factor ν of approximately 0.58–0.60, in good agreement with expectation. (The hydrodynamic radius, R_h, is proportional to M^{ν}; intrinsic viscosity is proportional to $M^{2\nu}$ for the free-draining chain, but proportional to $M^{3\nu-1}$ for the nonfree-draining ball.) Results for the low molecular weight region have been reported by Cleland,[32,35] Shimada and Matsumura,[34] Turner et al.,[36] Mendichi et al.,[37] and Hokputsa et al.,[38] who observed $M^{1.0-1.2}$ dependences. For the high molecular weight region, results have been reported by Laurent et al.[39] ($M^{0.78}$), Balazs[40] ($M^{0.80}$), Cleland and Wang[33] ($M^{0.816}$), Shimada and Matsumura[34] ($M^{0.76}$), Bothner et al.[41] ($M^{0.779}$), Fouissac et al.[42] ($M^{0.78}$), Gamini et al.[43] ($M^{0.81}$), Yanaki and Yamaguchi[44] ($M^{0.829}$), Berriaud et al.[45] ($M^{0.79}$), Takahashi et al.[46] ($M^{0.79}$), Mendichi et al.[37] ($M^{0.778}$), and Hokputsa et al.[38] ($M^{0.73}$). Hayashi et al.[47] obtained an intermediate dependence of $M^{0.92}$ in fitting data that spanned the two molecular weight ranges. Above a molecular weight of about 1×10^6, some reports[37,41] indicate a further decrease in exponent to 0.6, but this may be partly a result of the susceptibility of the very large coil to perturbation at nonzero shear rates. Thus for HA the form of the dependence of the intrinsic viscosity on molecular weight fits the predicted change from short extended chains to longer chains coiled into hydrodynamic spheres as the molecular weight increases.

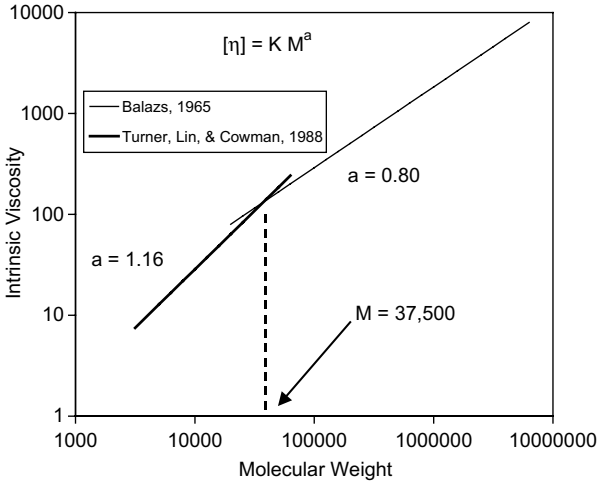

Figure 6. Experimental dependence of intrinsic viscosity on molecular weight for HA in 0.15 M NaCl solution. Note the different behavior of low and high molecular weight samples (Ref. 27).

Using the wormlike chain model, the change in exponent as a function of molecular weight can be explained in terms of a measure of the intrinsic stiffness of the chain, which is the persistence length. Various groups of researchers have fit the data to differing values of the persistence length. Values near 4–5 nm were determined by Cleland,[35,48] Hayashi and co-workers,[47,49] Tsutsumi and Norisuye,[50] Takahashi et al.,[46] Norisuye,[51] and Cowman and Matsuoka.[27] Higher values of 7–10 nm were obtained by Ghosh et al.,[52] Gamini et al.,[43] Fouissac et al.,[42] Milas et al.,[53] and Berriaud et al.[45] The discrepancy may reflect the contribution of polydispersity to the calculated value[46] and/or differing degrees of correction for excluded volume effects.

The usual practice in analysis of the intrinsic viscosity of HA includes a linear extrapolation of the reduced viscosity (η_{sp}/c) to zero concentration, thus assuming that only the first two terms of the viscosity equation (Eq. 1) are necessary, and the Huggins' constant is obtained from the slope. The theoretical value is 0.4. Reported values include 0.35–0.45 (Shimada and Matsumura[34]), 0.37–0.43 (Gamini et al.[43]), 0.33–0.57 (Fouissac et al.[54]), 0.396–0.427 (Berriaud et al.[55]), 0.35 (Yanaki and Yamaguchi[44]), 0.34–0.43 (Hayashi and co-workers[47,49]), 0.37–0.45 (Mo et al.[56]), 0.4 (Milas et al.[57]), and 0.34 (Krause et al.[58]). This is in accord with expectation.

Low molecular weight (M less than about 10^5) HA, especially in the size range expected to exist in the open, free-draining coil form in dilute solution (M less than about 4×10^4), has proven to be less amenable to simple analysis. When studied in 0.2 M phosphate buffer at 37 °C, the k' value was observed to be approximately zero.[34] On the other hand, there have been several reports[36,43,47] of the analysis of low molecular weight HA in 0.1–0.2 M NaCl solutions at or near 25 °C, which give anomalously high values for k', generally greater than 0.5 and as high as about 5. The reason for this deviation from theory is intermolecular self-association, which is notable only for low molecular weight HA. The association also leads to a commonly observed difficulty in filtering the solutions of low molecular weight HA before viscometric analysis, with significant sample loss.

Published measurements of the zero shear viscosity for HA in neutral salt solution as a function of concentration and molecular weight are in excellent agreement with the simple predictions of the four-term interaction equation (Eq. 1).

In dilute solution, when the product $c[\eta]$ is less than about 1, the specific viscosity is apparently dependent on $c[\eta]$ to a little more than the first power (Fig. 7).

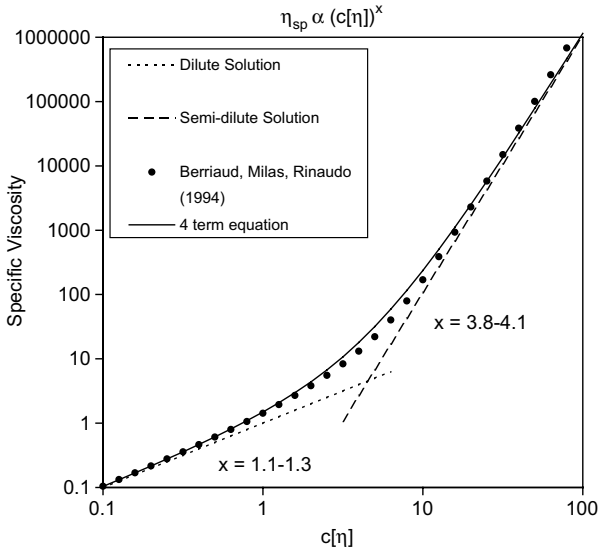

Figure 7. Dependence of the specific viscosity of HA solutions on the coil overlap factor. The slope of each straight segment is labeled with the range of values observed in the literature. The experimental data of Berriaud et al.[55] are compared with curves based on exponents cited in the literature and with the four-term equation (Eq. 1).

The data are often expressed in the literature in terms of the molecular weight, M, rather than $[\eta]$. We recall that $[\eta]$ is proportional to $M^{0.80}$ for the ball-like HA conformation, and can easily interconvert the variables. The actual range of exponents observed (probably strongly dependent on the exact range of $c[\eta]$ used in the data fit) show that η_{sp} depends on $c^{0.8-1.6}M^{1.0-1.5}$ in dilute solution, with exponents near 1.2 for c and 1.0 for M most commonly found.[54,56,58–62] This corresponds to $c^{1.2}\eta^{1.25}$ and shows that both the first and second power terms contribute in dilute solution.

In more concentrated solutions, when $c[\eta]$ is greater than about 10, the specific viscosity has been found[53,54,56–58,60–62] to depend on $c^{3.8-4.1}M^{3.3-4}$ equivalent to $c^{3.8-4.1}\eta^{4.1-5}$.

Berriaud et al.[55] have provided a polynomial fit to their extensive zero shear viscosity data covering the range from dilute to concentrated solution:

$$\eta_{sp} = c[\eta] + 0.42(c[\eta])^2 + 7.77 \times 10^{-3}(c[\eta])^{4.18} \quad (12)$$

A direct comparison of the four-term interaction equation (Eq. 1 with $k' = 0.4$) with the experiment-based equation 12 is given in Figure 7. There is seen to be an excellent agreement between the two. Thus the transition in specific viscosity from first power to fourth power dependence on concentration and intrinsic viscosity may be simply modeled in terms of intermolecular hydrodynamic coupling involving an increasing number of neighbors, up to a maximum of three neighbors. The high viscosity of HA solutions does not arise from the formation of a network stabilized by self-association of HA chains. Rather, the huge hydrodynamic volume of HA and simple transient intermolecular interactions, becoming more common as the molecular domains overlap, determine the viscosity. Assuming well-behaved solutions in which the HA is molecularly dissolved, the HA intrinsic viscosity (and thus its molecular weight) could be determined from a measurement of the zero shear viscosity measured at any concentration from dilute through semi-dilute regimes.

Numerous investigators have noted the strong shear rate dependence of HA solution viscosity. The shear thinning, as well as the change from viscous to elastic properties as a function of frequency of displacement in dynamic oscillatory measurements, are both related to the relaxation time of HA under the solution conditions used. The shear thinning and crossover phenomena have been noted by many groups.[6,33,54,57–61,63–68] For semi-dilute HA solutions, published dependencies of the relaxation time on concentration and molecular weight[57,58,61] generally show τ varies as c^2M^3 close to the predicted $c^2M^{3.4}$ (equal to $c^2[\eta]^3M$) dependence of the largest term in Eq. 6.

Published measurements of the elastic modulus are also in agreement with the predictions developed from the hydrodynamic interaction treatment. Thus Eq. 8 shows the value of G_e for semi-dilute solutions should depend on $c^2[\eta]/M$, or $c^2M^{-0.2}$. Experimental data for HA in semi-dilute solution[57,58,62] show G_e depends on $c^{2.0-2.8}M^0$.

6.2. HA solution viscosity under other conditions

The effects of certain environmental variables on solution viscosity are as expected for a semi-flexible polyelectrolyte. In a few other conditions, evidence for self-association has been reported.

The temperature dependence of the intrinsic viscosity of HA has been investigated by Cleland[69] and Fouissac et al.[54] Over the temperature range of 25–60 °C, the persistence length decreases, leading to a decrease in intrinsic viscosity. This reflects the increased population of high energy conformers at high temperatures. The bulk solution viscosity was confirmed to decrease as a result.[53,59] Recently, Hoefling et al.[70] found that the temperature dependence (25–65 °C) of the viscosity of semi-dilute HA solutions could be predicted from the expected change in intrinsic viscosity, using the four-term interaction equation (Eq. 1).

Addition of alkali similarly changes the population of conformers, possibly by eliminating interresidue hydrogen bonds as hydroxyl groups become ionized, making HA more contracted. As a result, the viscosity is dramatically reduced.[59,71,72] This effect is rapid and reversible, and not due to the slow cleavage of glycosidic linkages in alkali.[72]

Acid protonates carboxyl groups, decreasing intramolecular electrostatic repulsion, and reduces the intrinsic viscosity, in the absence of added salt.[33,48,73,74] In the presence of salt, and over a narrow acidic pH range, a marked enhancement of the viscosity is seen (see below).

Low ionic strength increases both intramolecular and intermolecular electrostatic repulsion, and increases the measured intrinsic viscosity in a manner expected for a flexible polyelectrolyte.[42,49,50,55,71,74–79]

There have been several still unverified reports of changes in the intrinsic viscosity of HA in the presence of potassium counterions instead of the usual sodium ions. A surprising pH-dependent transition, near neutral pH, was reported by Barrett and Harrington.[80] Using potassium phosphate buffers in the pH range 6.0–8.5 at an ionic strength of 0.1, these authors observed a dramatic drop in zero shear intrinsic viscosity as pH was decreased from 7.5 to 7.0. It should be noted that the concentration range used to extrapolate the reduced viscosity to zero concentration was quite high, opening the possibility that a small change in bulk viscosity due to aggregation could result in an erroneous estimation of the intrinsic viscosity. The phenomenon was reexamined by Balazs et al.,[81] but no change in intrinsic viscosity between pH 6 and 8 in potassium phosphate under the same conditions was observed. Sheehan et al.[82] made a detailed low shear viscometric study of HA in NaCl, KCl, and $CaCl_2$ solutions. The intrinsic viscosity was higher in NaCl than in KCl, and the solution viscosity in NaCl was also higher at all concentrations. Molecular weight determined by light scattering also was higher in NaCl. A sodium-dependent association was proposed, but this observation could not be repeated by others[83] for high molecular weight HA. (It should be noted, however, that Cowman et al.[84] used light scattering to show that low molecular weight HA segments reversibly associate in NaCl but not KCl.) HA in $CaCl_2$ had anomalous results, having aggregation like that in NaCl suggested by light scattering and intrinsic viscosity, but unusual shear thinning leading to a lower viscosity at finite concentrations. Takahashi and Ogino[85] studied the viscosity of sodium and potassium salts of HA in solutions containing no added salt from 30 to 50 °C. They confirmed the monotonic decrease in viscosity seen with increasing temperature for NaCl-containing solutions. At all temperatures, the solution of the potassium salt exhibited a lower viscosity than the sodium salt form.

A rheological study of mixtures of high and low molecular weight HA indicated that the fragments disrupted a network formed by the high molecular weight molecules,[86] but this work was refuted.[87]

Finally, there are some conditions for which marked changes in HA solution properties occur. The significant changes in the rheological properties suggest the HA chains enjoy specific intermolecular interactions. The viscoelastic putty state, adopted near pH 2.5 in the presence of physiological NaCl concentration, must reflect intermolecular association.[59,73,88] Other unusual structures must exist in mixed ethanol–water solvent at low pH, and a gel forms in that solvent in the presence of sufficient NaCl.[89–91]

7. Summary of experimental results from osmotic pressure analyses

There have been relatively few studies of the colloid osmotic pressure exerted by HA solutions. Notable among these are studies by Jensen and Marcker,[92] Laurent and Ogston,[93] Cleland and Wang,[33] Granger et al.,[94] and Bothner and Wik.[95] The osmotic pressure of HA solutions in the concentration range of 1–10 mg/mL is found to be markedly nonlinear, with the molecule exerting a far greater osmotic contribution than might be expected on the basis of the high molecular weight, since osmotic pressure measures the number of molecules in solution. Consideration of the nonideality contribution, however, makes it clear why HA exerts such a large effect: the molecular domain is large, and the molecules consequently interfere with each other, increasing the osmotic effect. Figure 8 shows a plot, calculated using Eq. 9, of the osmotic pressure for a solution of monodisperse HA with a molecular weight of 1×10^6. If only the first (ideal condition) term is included, the osmotic pressure is modest, but inclusion of the second and third terms greatly affects the osmotic pressure. The three term expression is compared in Figure 8 with experimental data taken from Laurent and Ogston.[93] The agreement is excellent, showing that the nonideality is entirely accounted for by consideration of simple hydrodynamic

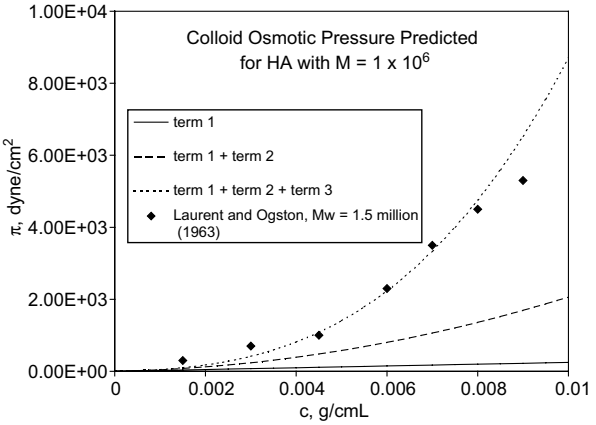

Figure 8. The colloid osmotic pressure of NaHA solutions (ionic strength 0.5, temperature 20.0 °C) observed experimentally by Laurent and Ogston,[93] in comparison with the predicted osmotic pressure resulting from intermolecular interactions (Eq. 9).

interaction between the large domains of the HA chains. The need for the third term explains why Cleland and Wang[33] found it useful to subtract a constant term for the third virial coefficient before plotting reduced osmotic pressure data using two terms. The second virial coefficient obtained in this way was approximately 2×10^{-3}, and decreased slightly with increasing molecular weight, as predicted by Eq. 10.

We may conclude that the available osmotic pressure data for HA can be interpreted as typical behavior for a high molecular weight semi-flexible polymer, analyzed over a broad concentration range.

8. Summary of experimental results from light scattering analyses

8.1. HA in neutral aqueous salt solutions

A number of papers report the use of elastic light scattering for the analysis of HA weight-average molecular weight. The work of Cleland and Wang[33] is notable in this regard. The second virial coefficient has been reported, and values near 2×10^{-3} mol mL g^{-2} are common for HA in 0.1–0.2 M NaCl,[31,43,96–98] with molecular weight dependence as given above, being smaller as molecular weight increases.[31,98] This is in agreement with prediction. Anomalously low or even negative second virial coefficients were found for short HA fragments, in accord with a proposed aggregation by the extended chains.[36]

Laurent and Gergely[99] showed that the angular dependence of the scattering was in accord with a random coil polymer configuration. Also from the angular dependence, the radius of gyration is found to depend on $M^{0.57–0.60}$, again as predicted.[31,37,39,42,46,50,98] There is less agreement on the persistence length of HA, which is calculated from the radius of gyration dependence on molecular weight using various approaches that differ in the manner in which excluded volume is treated. Thus the persistence length is reported to be near 4–5 nm[31,46,50,100] or 7–15 nm.[37,42,43,98] Takahashi et al.[31,46] make a strong case for the need to correct persistence lengths for the broad molecular weight distribution of the sample, thus correcting the persistence length from 9 to 4 nm.

8.2. HA in differing solvent conditions

In alkali, the HA chain contracts, possibly as a result of hydrogen bond breakage. Under these conditions, the radius of gyration and second virial coefficient decrease.[72,101] The possibility that HA associates in NaCl and $CaCl_2$ but not KCl was suggested by the light scattering studies of Sheehan et al.,[82] but have been disputed by Månsson et al.[83]

9. Summary of experimental results from diffusion coefficient analyses

Few studies have been performed to measure the diffusion coefficient of HA. One significant exception is the work of Wik and Comper,[102] who used the analytical ultracentrifuge to determine diffusion coefficients by boundary relaxation. More recently, the confocal FRAP method was elegantly employed by Hardingham and coworkers[103,104] to provide detailed analyses of the diffusion coefficient dependence on solution composition and temperature. The diffusion coefficient decreases with increasing HA concentration, with reduced ionic strength, and near pH 2.5. It increases with addition of divalent ions, addition of alkali, increase in temperature, addition of urea, or addition of ethanol. The expansion or shrinkage of the molecular domain with these perturbations seems to follow expectation. The authors point out that the data firmly establish the lack of a network for HA in physiological saline solution, even under quiescent conditions, which would be stabilized by chain–chain interactions, as had previously been proposed. This interpretation is in full agreement with the current understanding of the rheological properties of HA solutions.

10. Local conformation and dynamics of HA: nuclear magnetic resonance (NMR) spectroscopy

10.1. NMR studies of HA in neutral aqueous solution

HA has been rather extensively studied by NMR spectroscopy. Using ^{13}C NMR, both low and high molecular weight HA give clear spectra, as a result of the segmental mobility within the polymer. The resonances for individual carbons in the repeating disaccharide structure have been identified and assigned.[105–107] The chemical shifts of the resonances are as predicted on the basis of monosaccharide and disaccharide studies, and are independent of molecular weight, from polymer to hexasaccharide, disregarding the discrete resonances attributable to end effects in oligosaccharides.[107–109] The chemical shifts of HA carbons are similar in solution and in the solid state, although differences in chemical shift of linkage carbons suggest a conformational change upon dissolution, resulting from loss of stable hydrogen bonding between sugar residues.[110] A change in chemical shifts of the linkage carbons is also observed during shearing, which extends the molecular chain,[111] and by the chain expansion observed at low ionic strength.[108] The dynamics of segmental motion in HA in solution have been investigated by measuring longitudinal and transverse (T_1 and T_2) relaxation times, and the nuclear Overhauser enhancement (NOE) of the carbon resonances. Segmental motions on the nanosecond

time scale are observed.[109,112–114] There has been some discussion about the significance of the greater broadening of the carbonyl carbon of the acetamido group, and it has been proposed to arise from tertiary structure of HA aggregates, which may be disrupted by esterification of the spatially nearby carboxyl group.[115,116] However, the relaxation mechanism for this carbon is presumed to involve relaxation by a nearby proton (possibly the protons of the mobile acetamido methyl), and the precise connection with segmental motion is unresolved.[105,113] Shearing causes the resonance to broaden further, as the chain becomes extended and mobility is reduced.[111]

In HA oligosaccharides, the end residues differ in lacking one glycosidic linkage each, and the carbons near the missing linkage points are easily distinguishable in chemical shift.[107–109,114,117] Moreover, some carbons of penultimate residues in an oligosaccharide also show distinct chemical environments. The interior residues of oligosaccharides have similar dynamics to polymer residues, but the oligosaccharide ends tend to be more mobile. A detailed analysis of the relation between relaxation times and motional modes illuminated by molecular dynamics simulations has been presented by Letardi et al.,[118] and Furlan et al.,[119,120] and will not be discussed here.

The use of ^{1}H NMR for the study of HA oligosaccharides in aqueous solution has provided additional detail regarding local structure. The ring protons have chemical shifts and coupling constants consistent with the covalent structure and the $^{4}C_{1}$ ring conformation for both sugars.[107,121–123] The amide proton resonance has a chemical shift and coupling constant that indicate its approximately *trans* orientation with respect to the ring proton at C-2, and the lack of a direct hydrogen bond to the carboxylate group of the adjacent sugar.[122,124] ^{1}H–^{1}H NOE data suggest the acetamido group may be twisted even further away from the carboxylate group than the purely *trans* arrangement suggested above.[125] Nevertheless, the slow proton exchange rate of the amide proton with water protons suggest it may retain some hydrogen bonding to the carboxylate group, via a bridging water molecule.[126]

10.2. NMR studies of HA in perturbing environments

The chemical shifts and relaxation properties of the carbons in HA are little affected by moderate changes in ionic strength, except that the carbons of the (1→3) linkage show a small shift consistent with chain expansion at low ionic strength.[108] Divalent cations similarly cause a small shift in the (1→3) linkage carbons, consistent with chain contraction.[108] For HA polymer, significant line sharpening in the presence of Ca^{2+} was noted,[127] but has not been seen in HA segments of lower molecular weight.[108,112] Increasing temperature increases mobility, but no significant changes in interresidue coupling constants have been observed.[123,128] Alkali, already known to cause a major contraction of the HA domain in solution, causes sharpening of both ^{1}H and ^{13}C resonances, consistent with increased mobility.[105,112,121] The alkali effect is attributed to loss of interresidue hydrogen bonds, and thus a loss of a stiffening influence in the polymer at neutral pH.

Scott and Heatley used NMR extensively to investigate the properties of HA oligosaccharides in dimethyl sulfoxide, a solvent which can act as a hydrogen bond acceptor, but not a donor.[126,129–133] As a result, several intramolecular hydrogen bonds in HA are stable. A model incorporating three hydrogen bonds per disaccharide, stabilizing the conformations at both glycosidic linkages, has been proposed.[134] A similarity in conformation for HA in dimethyl sulfoxide solution and the fourfold helical form of HA in the solid state has been proposed on the basis of carbon chemical shift similarities.[110] A major stabilizing feature of the HA structure in dimethyl sulfoxide seems to be the hydrogen bond between the acetamido NH and the carboxyl group, since esterification of the carboxyl results in a more mobile chain structure in DMSO, and chemical shifts like that of HA in water.[135]

On the basis of all available NMR data for HA, the local conformation in aqueous solution may best be regarded as having the possibility of three different hydrogen bonds across the glycosidic linkages, but that these hydrogen bonds must be sufficiently short lived to maintain substantial segmental motion for the polymer on the nanosecond time scale.

11. Local conformation of HA: optical rotatory dispersion (ORD) and circular dichroism (CD) spectroscopy

11.1. HA in aqueous solution

Stone[136,137] was the first to publish the ORD and CD spectroscopic properties of HA in aqueous solution. Because interpretation of ORD spectra may be complicated by contributions from transitions centered at inaccessible wavelengths, only the CD spectra will be discussed here. A negative CD band centered near 210 nm was attributed primarily to the n–π* transition of the amide chromophore of the acetamido group, with a smaller contribution from the n–π* transition of the carboxyl(ate) chromophore. There was only low magnitude CD near 190 nm, where the π–π* transition of the amide chromophore was expected. Using vacuum ultraviolet CD, Cowman et al.[138] later showed that the π–π* transition of the amide chromophore at C-2 of the GlcNAc residue is strongly affected by the formation of glycosidic linkages at C-1 (which causes a large positive CD contribution) and at C-3 (causing a large negative CD

contribution), and that the linkage contributions are offsetting when both are present.

The 210 nm band was found to be much lower in intensity in HA oligosaccharides than in HA polymer, and this was attributed to the adoption of helical order by the polymer but not the short oligomers.[139] Later work showed that the intensity change was simply the result of discrete contributions from the end residues of the short oligomers, and that there was no apparent contribution from helical order.[140] (Note that this statement concerns only the interpretation of the CD spectra, and does not prove a lack of helical order.)

11.2. CD spectra of HA under perturbing conditions

Since HA solutions form a viscoelastic putty state at pH 2.5 in the presence of a physiological concentration of NaCl, the CD properties were examined at low pH. Salts were present only at very low concentration, to avoid the technical difficulty of handling the putty sample. Initial reports[139] of a strong positive CD band near 190 nm were difficult to reproduce,[141] but a weak positive band was shown to exist using vacuum ultraviolet CD instruments.[142,143] It has been attributed to a small noncooperative change in environment of the carboxyl chromophore upon protonation.

HA in the solid state gives a very different CD spectrum.[142] There is a strong negative CD band near 190 nm, attributed to the amide chromophore. Its great intensity is due to the more rigid environment in the solid, where the amide group may be hydrogen bonded to the carboxyl(ate) group across the β-(1→4) linkage.

An equally interesting change in optical properties occurs when acidic aqueous solutions of HA are mixed with ethanol, 1,4-dioxane, acetonitrile, or trifluoroethanol. Under these conditions, HA can gel. Park and Chakrabarti[89–91] reported the appearance of a large negative CD band near 190 nm, and a weak positive band near 225 nm. The CD changes were cooperatively eliminated at temperatures near 50 °C. Staskus and Johnson[143,144] provided an elegant and detailed examination of the effect, using vacuum ultraviolet CD. They found that short oligomers (less than nine disaccharides) of HA could not undergo the conformational change. For oligomers with 10–18 disaccharides, the changes were concentration dependent, whereas it was concentration-independent for longer chains. The concentration dependence of the transition for a 16 disaccharide fragment was fit by a monomer–dimer equilibrium with finite cooperativity. Thus self-association is proven for HA oligomers in aqueous–organic mixed solvents at pH near 2.5.

11.2.1. Change in the specific rotation of HA solution with urea. The specific rotation, $[\alpha]_D$, at 25 °C, measured by polarimetry of HA solution, is generally near −74°. Hirano and co-workers[145–147] showed that HA in 8 M urea had a specific rotation of approximately −17°. The altered HA could be isolated by gel filtration as a more compact form. Heating the altered sample to 85 °C, followed by slow cooling, caused reversion of the HA to the original specific rotation. The nature of this conformational change has not been established.

12. New insights from studies of HA on the surfaces: electron microscopy (EM) and atomic force microscopy (AFM)

The picture of HA conformation and properties that is obtained from most electron microscopic and atomic force microscopic studies is quite different than that indicated by physicochemical analyses of HA in neutral aqueous solution. When deposited on mica, shadowed, and studied under vacuum by EM, HA has a tremendous tendency to self-associate, forming networks of fibrils with diameters ranging from 2 to 5 nm to larger fibers up to 30 nm in diameter.[148–156] The same behavior is often seen using AFM for HA deposited on mica and studied under butanol or in air through a thin layer of water existing on the surface of the mica.[84,157–166] The network can be disrupted by complexing HA with protein, either specifically[151,155] or nonspecifically.[167] A marked appearance of helicity is found in HA complexed with the double globe fragment of proteoglycan core protein, which appears to spiral around the HA chain.[151]

The frequent observation of networks or fibrillar assemblies led Scott and co-workers to propose that HA exists in ordered assemblies of extended molecules in aqueous solution. That view is incompatible with the physicochemical data present above. However, the possibility that crowded physiological environments and mechanical forces could extend HA chains and favor ordered association under some conditions in vivo remains an interesting question (see below).

When HA solutions are deposited on the surfaces at low (usually 1–10 μg/mL) concentration, individual molecules can be imaged. The shape of the chain depends on its interactions with the surface.[164–166] HA deposited on mica prehydrated to develop an ordered water layer, or deposited on graphite, can be found in an extended form after extension by the force of a moving droplet of water across the surface ('molecular combing'). The molecule should recoil, but sufficiently strong interactions can form with the icelike water layer on mica or with graphite to inhibit recoil. This illustrates the dual hydrophilic and hydrophobic aspects of HA structure. When HA is deposited on freshly cleaved mica, lacking the preformed water layer, it becomes immersed in the water layer and can be imaged in more relaxed forms. The relaxed forms often have sections with a distinctly helical

appearance (Fig. 9A–C). This reflects the lowest energy conformation for HA, which is favored in the structured water environment. Because HA has an intrinsically low affinity for mica (which bears a negative charge from loss of potassium ions with cleavage), more condensed forms are often seen. The intramolecular condensation of HA proceeds through a pearl necklace form to rodlike forms with increasing degree of condensation (Fig. 9D–F). Additional intermolecular association can lead to fibrils formed from short rodlike chains or longer less perfectly condensed worms (Fig. 10A–B). Alternatively, chains extended by force can associate into ropelike fibrils in which the chains are twisted about each other and oriented in approximately the same direction as the fibrils (Fig. 10C–D). We have observed these structures under conditions leading to network formation, with the extended chains being pulled by two different junction points in the network.

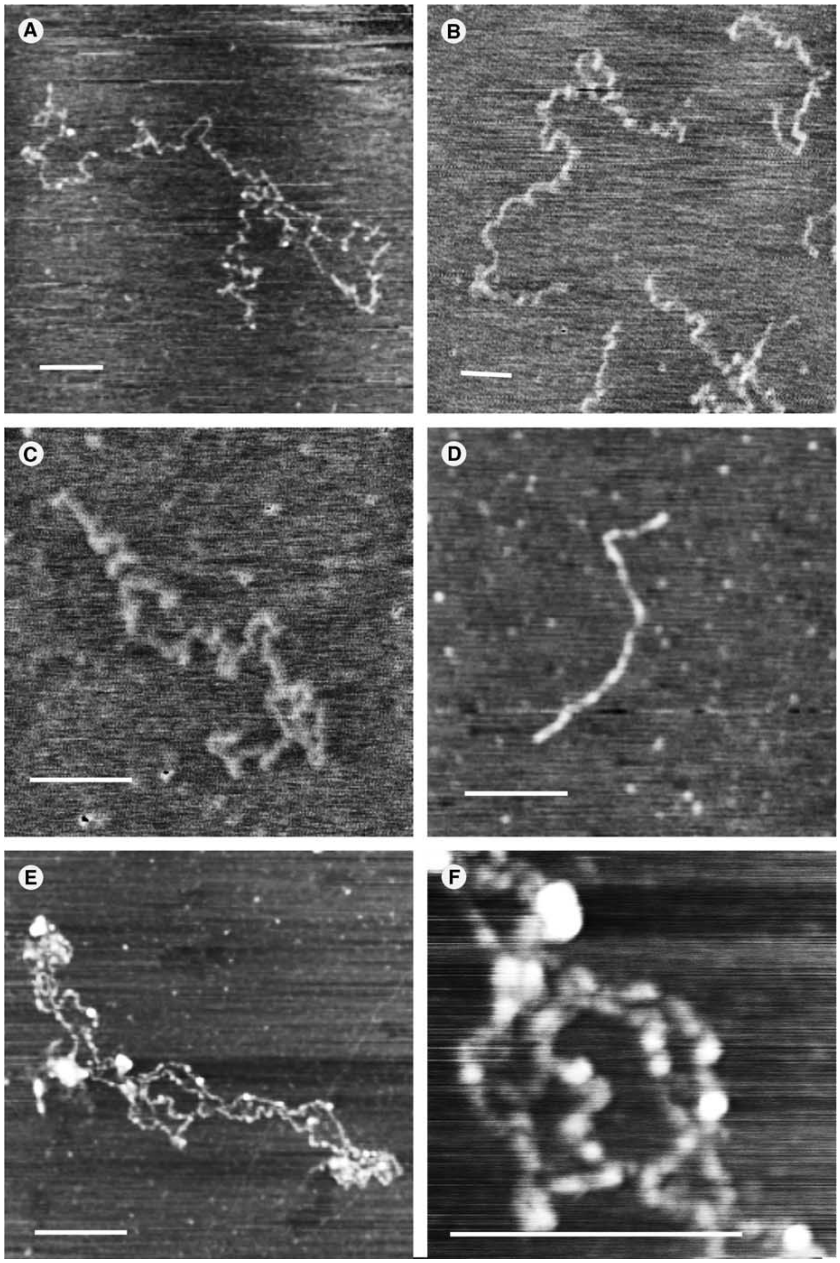

Figure 9. AFM images of HA deposited on mica, showing relaxed and partially condensed hyaluronan chains. Image A is from Ref. 162. Images B, C, E, F are from Ref. 165. Bar = 250 nm.

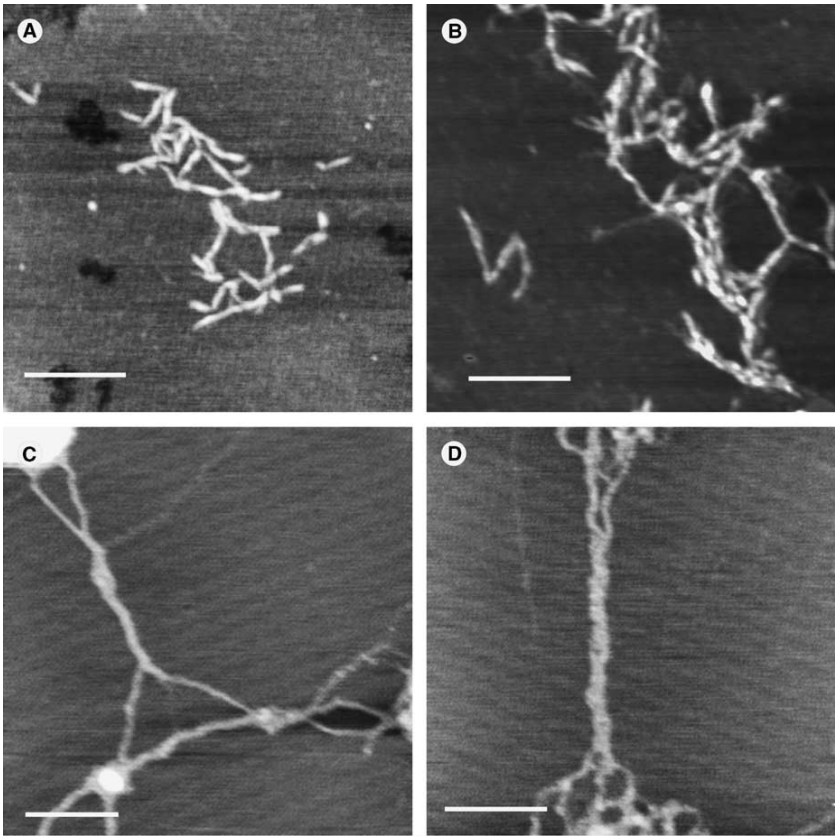

Figure 10. AFM images of HA showing condensed chain aggregation (A, B) and extended chain aggregation (C, D) into fibrils. Images are from Ref. 165. Bar = 250 nm.

13. The importance of counterion-mediated polyelectrolyte interactions

The mechanism for ordered intramolecular condensation is explained by theories for counterion-mediated interaction between polyelectrolytes. The solubility of a polyelectrolyte is enhanced by the mixing entropy of the charged polymer and its counterions with solvent, by favorable enthalpic interactions between the polymer and solvent, by the entropic contributions favoring a statistically random polymer chain configuration, and by electrostatic repulsion between charged groups on the polymer. Intramolecular condensation of a polyelectrolyte chain *in solution* is thought to occur when the polymer concentration is dilute and one of three types of conditions are met. These include (1) near complete neutralization of polyelectrolyte charges by multivalent (+3 or higher) ions, (2) low dielectric constant (e.g., in aqueous–organic mixed solvents, or in the partially structured water near hydrophilic surfaces) and sufficient concentrations of (usually) divalent ions, or (3) high excluded volume, due to the presence of other species like polyethylene glycol, and sufficient mono- or higher valent counterion concentrations to minimize repulsion. The effective neutralization of the polyelectrolyte charges in each case is almost but not quite complete. The counterions are localized to the immediate vicinity of the polyelectrolyte chain, but are not generally site bound. There are several models to explain the appearance of an attractive electrostatic force between segments of like-charged polyelectrolytes. Among these are (1) an attraction arising from correlated fluctuations in position of condensed counterions on the polyelectrolytes[168,169] (analogous to induced dipole-induced dipole interactions), (2) sharing of counterions between chain segments, leading to an increased entropy for the counterions relative to their more restricted locations in a thin shell surrounding each separate chain segment,[170] and (3) matching of lattices of counterions formed around separate chain segments, so that holes in one lattice are matched by counterions in a second lattice.[171]

In addition to the attractive electrostatic interaction, a hydration contribution to polyelectrolyte condensation has been proposed. Highly hydrophilic polymers can structure the water in their immediate environment. In a manner conceptually similar to the hydrophobic effect, the hydration effect results in increased entropy for

water molecules freed by association of two polymer segments. The associated polymer surfaces can retain one or more layers of water bridging between the polymers. An interesting aspect of this contribution to polyelectrolyte condensation is that chaotropic ions that disrupt bulk water structure will favor polymer condensation, because the entropic difference between bound water and bulk water is increased.

The effect of surfaces such as mica or graphite on the condensation of polyelectrolytes is less well understood. By consideration of the driving forces for condensation in solution, it may be proposed that condensation would be favored if the polyelectrolyte is poorly solvated by the structured water at the surface, if counterion condensation leads to a more complete charge neutralization, if reduction in the effective dielectric constant increases the strength of attractive interactions due to correlated ion fluctuations, and if the polyelectrolyte–polyelectrolyte interactions are more favorable than surface–polyelectrolyte interactions.

14. Perspectives on HA in physiological environments

The observations of apparently helical chains, ordered condensates and fibrillar aggregates of HA on mica surfaces, and the predictions of the theories for counterion-mediated polyelectrolyte attraction, suggest that HA conformation and interactions in specific physiological and pathological environments may be more complicated than the simple random coil model. Here we propose two special types of behavior that may exist.

15. Does the relaxed form of HA have a helical bias?

Relaxed HA chains trapped in a water layer on mica have the appearance of weakly helical conformations. A similar helical tendency had been previously noted for HA complexed with the double globe fragment of cartilage proteoglycan core protein, upon imaging on mica by EM.[151] Although on a different length-scale, pseudo-helical molecular conformations, lacking long-range cooperative interactions, had been proposed in the past for other polysaccharides in solution. For example, local helical ordering in the amylose chain conformation was described in the pioneering work of Brant and co-workers,[172] using the Monte Carlo method to effectively generate representative snapshots of coiled chains. For HA, theoretical molecular dynamics and molecular mechanics calculations also suggest the accessibility of linkage conformations that can lead to wide left- or right-handed helices having 3–10 disaccharides per turn and low rise per residue.[173,174] The role of water is considered very important in determining the conformations adopted by HA,[175] and this raises the concern that the artificial environment on a mica surface, hydrated or not, is different than the bulk water environment. There is no proof for a weakly helical HA conformation in aqueous solution, even if in equilibrium with other conformations leading to an overall random coil form, although it would be consistent with all available data, and is the best interpretation for the induced optical activity seen in HA complexed with the metachromatic dye acridine orange.[176] It is interesting to note that certain bacterial polysaccharides apparently adopt conformations with overall random coil structure, but containing occasional segments of helical order, based on small differences in free energy among multiple conformations. The helical segments of the polysaccharides are thought to be recognized by antibodies as foreign, while fragments too short to form the helix are not recognized.[177] This is proposed to be a mechanism by which small oligosaccharides of similar covalent structure, native to the host tissue, remain nonantigenic. It may be speculated that the differing physiological effects of high and low molecular weight HA could also relate to the statistical adoption of conformational order by chain segments within the polymer, and resulting differences in binding interactions with proteins. The more crowded environment inside cells or at cell surfaces may also favor the lower energy conformation, in the same way that the structured solvent at mica surfaces does.

16. Do condensed and/or associated forms of HA exist under special conditions?

In the analysis of HA by hydrodynamic and spectroscopic methods, several special circumstances were found to cause significant conformational changes and/or self-association of HA. One of these is the gel formed at pH 2.5 in mixed aqueous/organic solvents. A sufficient concentration of NaCl is required for the transformation. In view of the theoretical explanations for polyelectrolyte condensation or association described above, the association of HA is expected under the conditions of low dielectric constant of the mixed solvent and nearly complete charge neutralization of HA at pH 2.5. (The intrinsic pK_a of HA is 3.2.) Even without the addition of an alcohol, HA at pH 2.5, in the presence of physiological concentrations of NaCl, forms a viscoelastic putty. Neither higher nor lower pH exerts the same effect. We may speculate that the attractive electrostatic interaction, which is operative only under a narrow range of effective charge neutralization of the polymer (approx. 90%), is responsible for the observed intermolecular association. In both of the above cases, we predict intramolecular condensation of HA chains if the solutions were sufficiently dilute.

The X-ray diffraction study leading to the identification of a double helical form of HA used ionic conditions that can also be understood to lead to self-association of the polyelectrolyte chain. The double helix of HA was produced[22] from solutions of low pH with K^+ counterions, or at neutral pH in the presence of NH_4^+ or Rb^+ or Cs^+. As noted by those authors, the counterions favoring the double helix are water structure breakers, so that association may in this case be favored by the hydration force previously described.

Trivalent lanthanide ions have recently been shown to precipitate HA from nondilute solutions.[178] At appropriate concentrations, the trivalent ions can cause the near complete charge neutralization of HA, favoring an attractive electrostatic interaction. The temperature dependence of the association (greater association at higher temperature) is also compatible with a stabilizing contribution from the hydration force.

The rigidity of short HA chains favors intermolecular interaction over intramolecular condensation at all concentrations. We have previously shown that short HA segments (with molecular weight less than about 15–20×10^3) show light scattering evidence of intermolecular association in aqueous NaCl solution.[36] Longer HA chains do not show this effect. One possible explanation is that longer chains undergo transient intramolecular association. Alternatively, the entropic cost of intermolecular association by high molecular weight HA, under conditions of high residual negative charge and good solvent, may be too high.

We anticipate that we will find physiological conditions of high excluded volume, multivalent cationic binding species, and structured water with a low dielectric constant that could favor ordered condensation or aggregation. The many biological functions of HA may yet be shown to depend on its conformational diversity.

Acknowledgements

Portions of this work were supported by Biomatrix, Inc., Genzyme Biosurgery, and The Matrix Biology Institute. The authors thank Dr. Endre A. Balazs for his support and continuing interest in the fundamental properties of hyaluronan.

References

1. Lee, H. G.; Cowman, M. K. *Anal. Biochem.* **1994**, *219*, 278–287.
2. Armstrong, S. E.; Bell, D. R. *Anal. Biochem.* **2002**, *308*, 255–264.
3. Li, M.; Rosenfeld, L.; Vilar, R. E.; Cowman, M. K. *Arch. Biochem. Biophys.* **1997**, *341*, 245–250.
4. Balazs, E. A. The Physical Properties of Synovial Fluid and the Special Role of Hyaluronic Acid. In *Disorders of the Knee,* 2nd ed.; Helfet, A., Ed. 1982; JB Lippincott Company: Philadelphia; pp 61–74.
5. Dahl, L. B.; Dahl, I. M. S.; Engstrom-Laurent, A.; Granath, K. *Ann. Rheum. Dis.* **1985**, *44*, 817–822.
6. Balazs, E. A. *Univ. Mich. Med. Ctr. J. (Suppl.)* **1968**, *22*, 255–259.
7. Balazs, E. A.; Denlinger, J. L. *J. Equine Vet. Sci.* **1985**, *5*, 217–228.
8. Laurent, T. C.; Laurent, U. B. G.; Fraser, J. R. *Immunol. Cell Biol.* **1996**, *74*, A1–A7.
9. Tammi, M. I.; Day, A. J.; Turley, E. A. *J. Biol. Chem.* **2002**, *277*, 4581–4584.
10. Day, A. J.; Prestwich, G. D. *J. Biol. Chem.* **2002**, *277*, 4585–4588.
11. Turley, E. A.; Noble, P. W.; Bourguignon, L. Y. W. *J. Biol. Chem.* **2002**, *277*, 4589–4592.
12. Toole, B. P.; Wight, T. N.; Tammi, M. I. *J. Biol. Chem.* **2002**, *277*, 4593–4596.
13. Hascall, V. C.; Majors, A. K.; de la Motte, C. A.; Evanko, S. P.; Wang, A.; Drazba, J. A.; Strong, S. A.; Wight, T. N. *Biochim. Biophys. Acta* **2004**, *1673*, 2–12.
14. de la Motte, C. A.; Hascall, V. C.; Drazba, J.; Bandyopadhyay, S. K.; Strong, S. A. *Am. J. Pathol.* **2003**, *163*, 121–133.
15. Majors, A. K.; Austin, R. C.; de la Motte, C. A.; Pyeritz, R. E.; Hascall, V. C.; Kessler, S. P.; Sen, G.; Strong, S. A. *J. Biol. Chem.* **2003**, *278*, 47223–47231.
16. Lapčık, L., Jr.; Lapčık, L.; DeSmedt, S.; Demeester, J.; Chabreček, P. *Chem. Rev.* **1998**, *98*, 2663–2684.
17. Hardingham, T. E. Solution Properties of Hyaluronan. In *Chemistry and Biology of Hyaluronan*; Garg, H. G., Hales, C. A., Eds.; Elsevier: Amsterdam, 2004; pp 1–19.
18. Guss, J. M.; Hukins, D. W. L.; Smith, P. J. C.; Winter, W. T.; Arnott, S.; Moorhouse, R.; Rees, D. A. *J. Mol. Biol.* **1975**, *95*, 359–384.
19. Winter, W. T.; Smith, P. J. C.; Arnott, S. *J. Mol. Biol.* **1975**, *99*, 219–235.
20. Winter, W. T.; Arnott, S. *J. Mol. Biol.* **1977**, *117*, 761–784.
21. Sheehan, J. K.; Atkins, E. D. T. *Int. J. Biol. Macromol.* **1983**, *5*, 215–221.
22. Sheehan, J. K.; Gardner, K. H.; Atkins, E. D. T. *J. Mol. Biol.* **1977**, *117*, 113–135.
23. Arnott, S.; Mitra, A. K.; Ragunathan, S. *J. Mol. Biol.* **1983**, *169*, 861–872.
24. Kwei, T. K.; Nakazawa, M.; Matsuoka, S.; Cowman, M. K.; Okamoto, Y. *Macromolecules* **2000**, *33*, 235–236.
25. Matsuoka, S.; Cowman, M. K. *Polymer* **2002**, *43*, 3447–3453.
26. Matsuoka, S.; Cowman, M. K. Viscosity of Polymer Solutions Revisited. In *Hyaluronan*; Kennedy, J. F., Phillips, G. O., Williams, P. A., Eds.; Woodhead: Cambridge, 2002; pp 79–88.
27. Cowman, M. K.; Matsuoka, S. The Intrinsic Viscosity of Hyaluronan. In *Hyaluronan*; Kennedy, J. F., Phillips, G. O., Williams, P. A., Eds.; Woodhead: Cambridge, 2002; 75–78.
28. Cowman, M. K.; Mendichi, R. Methods for Determination of Hyaluronan Molecular Weight. In *Chemistry and Biology of Hyaluronan*; Garg, H. G., Hales, C. A., Eds.; Elsevier: Amsterdam, 2004; pp 41–69.
29. Patel, S. S.; Takahashi, K. M. *Macromolecules* **1992**, *25*, 4382–4391.
30. Burchard, W. *Biomacromolecules* **2001**, *2*, 342–353.
31. Takahashi, R.; Al-Assaf, S.; Williams, P. A.; Kubota, K.; Okamoto, A.; Nishinari, K. *Biomacromolecules* **2003**, *4*, 404–409.

32. Cleland, R. L. Molecular Weight Distribution in Hyaluronic Acid. In *Chemistry and Molecular Biology of the Intercellular Matrix*; Balazs, E. A., Ed.; Academic: New York, 1970; pp 733–742.
33. Cleland, R. L.; Wang, J. L. *Biopolymers* **1970**, *9*, 799–810.
34. Shimada, E.; Matsumura, G. *J. Biochem.* **1975**, *78*, 513–517.
35. Cleland, R. L. *Biopolymers* **1984**, *23*, 647–666.
36. Turner, R. E.; Lin, P.; Cowman, M. K. *Arch. Biochem. Biophys.* **1988**, *265*, 484–495.
37. Mendichi, R.; Šoltés, L.; Giacometti Schieroni, A. *Biomacromolecules* **2003**, *4*, 1805–1810.
38. Hokputsa, S.; Jumel, K.; Alexander, C.; Harding, S. E. *Carbohydr. Polym.* **2003**, *52*, 11–117.
39. Laurent, T. C.; Ryan, M.; Pietruszkiewicz, A. *Biochim. Biophys. Acta* **1960**, *42*, 476–485.
40. Balazs, E. A. Amino sugar-containing macromolecules in the tissues of the eye and the ear. In *The Amino Sugars: The Chemistry and Biology of Compounds Containing Amino Sugars*; Balazs, E. A., Jeanloz, R. W., Eds.; Academic: New York, 1965; Vol. 2A, pp 401–460.
41. Bothner, H.; Waaler, T.; Wik, O. *Int. J. Biol. Macromol.* **1988**, *10*, 287–291.
42. Fouissac, E.; Milas, M.; Rinaudo, M.; Borsali, R. *Macromolecules* **1992**, *25*, 5613–5617.
43. Gamini, A.; Paoletti, S.; Zanetti, F. Chain Rigidity of Polyuronates: Static Light Scattering of Aqueous Solutions of Hyaluronate and Alginate. In *Laser Light Scattering in Biochemistry*; Harding, S. E., Satelle, D. B., Bloomfield, V. A., Eds.; Royal Society of Chemistry: Cambridge, 1992; pp 294–311.
44. Yanaki, T.; Yamaguchi, M. *Chem. Pharm. Bull.* **1994**, *42*, 1651–1654.
45. Berriaud, N.; Milas, M.; Rinaudo, M. Characterization and Properties of Hyaluronic Acid (Hyaluronan). In *Polysaccharides in Medicine and Technology*; Severian, D., Ed.; Marcel Dekker: New York, 1998; pp 313–334.
46. Takahashi, R.; Kubota, K.; Kawada, M.; Okamoto, A. *Biopolymers* **1999**, *50*, 87–98.
47. Hayashi, K.; Tsutsumi, K.; Nakajima, F.; Norisuye, T.; Teramoto, A. *Macromolecules* **1995**, *28*, 3824–3830.
48. Cleland, R. L. *Arch. Biochem. Biophys.* **1977**, *180*, 57–68.
49. Hayashi, K.; Tsutsumi, K.; Norisuye, T.; Teramoto, A. *Polym. J.* **1996**, *28*, 922–928.
50. Tsutsumi, K.; Norisuye, T. *Polym. J.* **1998**, *30*, 345–349.
51. Norisuye, T. Conformation and Solution Properties of Water-Soluble Polysaccharides: Case Study of Hyaluronic Acid. In *Hydrocolloids—Part 2*; Nishinari, K., Ed.; Elsevier, 2000; pp 311–320.
52. Ghosh, S.; Li, X.; Reed, C. E.; Reed, W. F. *Biopolymers* **1990**, *30*, 1101–1112.
53. Milas, M.; Roure, I.; Berry, G. C. *J. Rheol.* **1996**, *40*, 1155–1166.
54. Fouissac, E.; Milas, M.; Rinaudo, M. *Macromolecules* **1993**, *26*, 6945–6951.
55. Berriaud, N.; Milas, M.; Rinaudo, M. *Int. J. Biol. Macromol.* **1994**, *16*, 137–142.
56. Mo, Y.; Takaya, T.; Nishinari, K.; Kubota, K.; Okamoto, A. *Biopolymers* **1999**, *50*, 23–34.
57. Milas, M.; Rinaudo, M.; Roure, I.; Al Assaf, S.; Phillips, G. O.; Williams, P. A. *Biopolymers* **2001**, *59*, 191–204.
58. Krause, W. E.; Bellomo, E. G.; Colby, R. H. *Biomacromolecules* **2001**, *2*, 65–69.
59. Morris, E. R.; Rees, D. A.; Welsh, E. J. *J. Mol. Biol.* **1980**, *138*, 383–400.
60. Yanaki, T.; Yamaguchi, T. *Biopolymers* **1990**, *30*, 415–425.
61. Yu, L. P.; Burns, J. W.; Shiedlin, A.; Guo, Y.; Jankowski, T.; Pradipasena, P.; Rha, C. Rheological Characteristics of Microbially Derived Sodium Hyaluronate. In *Harnessing Biotechnol. 21st Century, Proc. Int. Biotechnol. Symp. Expo., 9th*; Ladisch, M. R., Bose, A., Eds.; ACS: Washington, DC, 1992; pp 80–84.
62. DeSmedt, S. C.; Dekeyser, P.; Ribitsch, V.; Lauwers, A.; Demeester, J. *Biorheology* **1993**, *30*, 31–41.
63. Ogston, A. G.; Stanier, J. E. *Biochem. J.* **1951**, *49*, 585–590.
64. Balazs, E. A.; Sundblad, L. *Acta Soc. Med. Upsaliensis* **1959**, *64*, 137–146.
65. Gibbs, D. A.; Merrill, E. W.; Smith, K. A.; Balazs, E. A. *Biopolymers* **1968**, *6*, 777–791.
66. Balazs, E. A.; Gibbs, D. A. The Rheological Properties and Biological Function of Hyaluronic Acid. In *Chemistry and Molecular Biology of the Intercellular Matrix*; Balazs, E. A., Ed.; Academic: New York, 1970; pp 1241–1253.
67. Tirtaatmadja, V.; Boger, D. V.; Fraser, J. R. E. *Rheol. Acta* **1984**, *23*, 311–321.
68. Lang, E.; Mark, D.; Miller, F. A.; Miller, D.; Wik, O. *Acta Ophthalmol.* **1984**, *102*, 1079–1082.
69. Cleland, R. L. *Biopolymers* **1979**, *18*, 1821–1828.
70. Hoefling, J. M.; Cowman, M. K.; Matsuoka, S.; Balazs, E. A. Temperature Effect on the Dynamic Rheological Characteristics of Hyaluronan, Hylan A, and Synvisc®. In *Hyaluronan*; Kennedy, J. F., Phillips, G. O., Williams, P. A., Eds.; Woodhead: Cambridge, 2002; pp 103–108.
71. Blix, G.; Snellman, O. *Arkiv für Kemi, Mineralogi o. Geologi.* **1945**, *19A*, 1–19.
72. Mathews, M. B.; Decker, L. *Biochim. Biophys. Acta* **1977**, *498*, 259–263.
73. Pigman, W.; Hawkins, W.; Gramling, E.; Rizvi, S.; Holley, H. L. *Arch. Biochem. Biophys.* **1960**, *89*, 184–193.
74. Cleland, R. L. *Biopolymers* **1968**, *6*, 1519–1529.
75. Madinaveitia, J.; Quibell, T. H. H. *Biochemistry* **1940**, *34*, 625–631.
76. Balazs, E. A.; Laurent, T. C. *J. Polym. Sci.* **1951**, *6*, 665–668.
77. Ribitsch, G.; Schurz, J.; Ribitsch, V. *Coll. Polym. Sci.* **1980**, *258*, 1322–1334.
78. Milas, M.; Rinaudo, M.; Borsali, R. *Ciencia e Cultura* **1993**, *45*, 46–48.
79. Rinaudo, M.; Roure, I.; Milas, M.; Malovikova, A. *Int. J. Polym. Anal. Charact.* **1997**, *4*, 57–69.
80. Barrett, T. W.; Harrington, R. E. *Biopolymers* **1977**, *16*, 2167–2188.
81. Balazs, E. A.; Cowman, M. K.; Briller, S. O.; Cleland, R. L. *Biopolymers* **1983**, *22*, 589–591.
82. Sheehan, J. K.; Arundel, C.; Phelps, C. F. *Int. J. Biol. Macromol.* **1983**, *5*, 222–228.
83. Månsson, P.; Jacobsson, Ö.; Granath, K. A. *Int. J. Biol. Macromol.* **1985**, *7*, 30–32.
84. Cowman, M. K.; Liu, J.; Li, M.; Hittner, D. M.; Kim, J. S. Hyaluronan Interactions: Self, Water, Ions. In *The Chemistry, Biology, and Medical Applications of Hyaluronan and its Derivatives*; Laurent, T. C., Ed.; Portland: London, 1998; pp 17–24.
85. Takahashi, S.; Ogino, K. *Nihon Reoroji Gakkaishi* **1997**, *25*, 143–148.
86. Welsh, E. J.; Rees, D. A.; Morris, E. R.; Madden, J. K. *J. Mol. Biol.* **1980**, *138*, 375–382.
87. Fujii, K.; Kawata, M.; Kobayashi, Y.; Okamoto, A.; Nishinari, K. *Biopolymers* **1996**, *38*, 583–591.

88. Balazs, E. A. *Fed. Proc.* **1966**, *25*, 1817–1822.
89. Park, J. W.; Chakrabarti, B. *Biopolymers* **1977**, *16*, 2807–2809.
90. Park, J. W.; Chakrabarti, B. *Biopolymers* **1978**, *17*, 1323–1333.
91. Park, J. W.; Chakrabarti, B. *Biochim. Biophys. Acta* **1978**, *541*, 263–269.
92. Jensen, C. E.; Marcker, K. *Acta Chem. Scand.* **1958**, *12*, 855–860.
93. Laurent, T. C.; Ogston, A. G. *Biochem. J.* **1963**, *89*, 249–253.
94. Granger, H. J.; Laine, S. H.; Laine, G. A. *Microcirc. Endothel. Lymph.* **1985**, *2*, 85–105.
95. Bothner, H.; Wik, O. Rheology of intraocular solutions. In *Viscoelastic Materials. Basic Science and Clinical Applications*; Rosen, E. S., Ed.; Pergamon: London, 1989; pp 53–70.
96. Silver, F. H.; Swann, D. A. *Int. J. Biol. Macromol.* **1982**, *4*, 425–429.
97. Terbojevich, M.; Cosani, A.; Palumbo, M. *Carbohydr. Res.* **1986**, *149*, 363–377.
98. Mendichi, R.; Giacometti Schieroni, A.; Grassi, C.; Re, A. *Polymer* **1998**, *39*, 6611–6620.
99. Laurent, T. C.; Gergely, J. *J. Biol. Chem.* **1955**, *212*, 325–333.
100. Norisuye, T.; Tsuboi, A.; Teramoto, A. *Polym. J.* **1996**, *28*, 357–361.
101. Ghosh, S.; Kobal, I.; Zanette, D.; Reed, W. F. *Macromolecules* **1993**, *26*, 4685–4693.
102. Wik, K.-O.; Comper, W. D. *Biopolymers* **1982**, *21*, 583–599.
103. Gribbon, P.; Heng, B. C.; Hardingham, T. E. *Biophys. J.* **1999**, *77*, 2210–2216.
104. Gribbon, P.; Heng, B. C.; Hardingham, T. E. *Biochem. J.* **2000**, *350*, 329–335.
105. Bociek, S. M.; Darke, A. H.; Welti, D.; Rees, D. A. *Eur. J. Biochem.* **1980**, *109*, 447–456.
106. Inoue, Y.; Nagasawa, K. *Carbohydr. Res.* **1985**, *141*, 99–110.
107. Toffanin, R.; Kvam, B. J.; Flaibani, A.; Atzori, M.; Biviano, F.; Paoletti, S. *Carbohydr. Res.* **1993**, *245*, 113–128.
108. Cowman, M. K.; Hittner, D. M.; Feder-Davis, J. *Macromolecules* **1996**, *29*, 2894–2902.
109. Cavalieri, F.; Chiessi, E.; Paci, M.; Paradossi, G.; Flaibani, A.; Cesàro, A. *Macromolecules* **2001**, *34*, 99–109.
110. Feder-Davis, J.; Hittner, D. M.; Cowman, M. K. Comparison of solution and solid-state structures of sodium hyaluronan by ^{13}C NMR spectroscopy. In *Water-soluble Polymers: Synthesis, Solution Properties and Applications*; Shalaby, S. W., McCormick, C. L., Butler, G. B., Eds., ACS Symposium Series, American Chemical Society: Washington, DC, 1991; 467, pp 493–501.
111. Fischer, E.; Callaghan, P. T.; Heatley, F.; Scott, J. E. *J. Mol. Struct.* **2002**, *602–603*, 303–311.
112. Hofmann, H.; Schmut, O.; Sterk, H.; Pölzler, H. *Int. J. Biol. Macromol.* **1983**, *5*, 229–232.
113. Naji, L.; Kaufmann, J.; Huster, D.; Schiller, J.; Arnold, K. *Carbohydr. Res.* **2000**, *327*, 439–446.
114. Cowman, M. K.; Feder-Davis, J.; Hittner, D. M. *Macromolecules* **2001**, *34*, 110–115.
115. Scott, J. E.; Heatley, F. *Proc. Natl. Acad. Sci. U.S.A.* **1999**, *96*, 4850–4855.
116. Scott, J. E.; Heatley, F. *Biomacromolecules* **2002**, *3*, 547–553.
117. Donati, A.; Magnani, A.; Bonechi, C.; Barbucci, C.; Rossi, C. *Biopolymers* **2001**, *59*, 434–445.
118. Letardi, S.; La Penna, G.; Chiessi, E.; Perico, A.; Cesàro, A. *Macromolecules* **2002**, *35*, 286–300.
119. Furlan, S.; La Penna, G.; Perico, A.; Cesàro, A. *Macromolecules* **2004**, *37*, 6197–6209.
120. Furlan, S.; La Penna, G.; Perico, A.; Cesàro, A. *Carbohydr. Res.* **2005**, *340*, doi:10.1016/j.carres.2005.01.030.
121. Welti, D.; Rees, D. A.; Welsh, E. J. *Eur. J. Biochem.* **1979**, *94*, 505–514.
122. Livant, P.; Rodén, L.; Krishna, N. R. *Carbohydr. Res.* **1992**, *237*, 271–281.
123. Sicińska, W.; Adams, B.; Lerner, L. *Carbohydr. Res.* **1993**, *242*, 29–51.
124. Cowman, M. K.; Cozart, D.; Nakanishi, K.; Balazs, E. A. *Arch. Biochem. Biophys.* **1984**, *230*, 203–212.
125. Holmbeck, S. M. A.; Petillo, P. A.; Lerner, L. E. *Biochemistry* **1994**, *33*, 14246–14255.
126. Heatley, F.; Scott, J. E. *Biochem. J.* **1988**, *254*, 489–493.
127. Napier, M. A.; Hadler, N. M. *Proc. Natl. Acad. Sci. U.S.A.* **1978**, *75*, 2261–2265.
128. Sicińska, W.; Lerner, L. E. *Carbohydr. Res.* **1996**, *286*, 151–159.
129. Heatley, F.; Scott, J. E.; Casu, B. *Carbohydr. Res.* **1979**, *72*, 13–23.
130. Heatley, F.; Scott, J. E.; Jeanloz, R. W.; Walker-Nasir, E. *Carbohydr. Res.* **1982**, *99*, 1–11.
131. Scott, J. E.; Heatley, F.; Moorcroft, D.; Olavesen, A. H. *Biochem. J.* **1981**, *199*, 829–832.
132. Scott, J. E.; Heatley, F.; Hull, W. E. *Biochem. J.* **1984**, *220*, 197–205.
133. Scott, J. E.; Heatley, F. *Biochem. J.* **1982**, *207*, 139–144.
134. Scott, J. E. Secondary Structures in Hyaluronan Solutions: Chemical and Biological Implications. In *The Biology of Hyaluronan*; Ciba Foundation Symposium 143, Wiley: Chichester, 1989; pp 6–20.
135. Kvam, B. J.; Atzori, M.; Toffanin, R.; Paoletti, S.; Biviano, F. **1992**, *230*, , pp 1–13.
136. Stone, A. L. *Biopolymers* **1969**, *7*, 173–188.
137. Stone, A. L. *Biopolymers* **1971**, *10*, 739–751.
138. Cowman, M. K.; Bush, C. A.; Balazs, E. A. *Biopolymers* **1983**, *22*, 1319–1334.
139. Chakrabarti, B.; Balazs, E. A. *J. Mol. Biol.* **1973**, *78*, 135–141.
140. Cowman, M. K.; Balazs, E. A.; Bergmann, C. W.; Meyer, K. *Biochemistry* **1981**, *20*, 1379–1385.
141. Balazs, E. A.; McKinnon, A. A.; Morris, E. R.; Rees, D. A.; Welsh, E. J. *J. Chem. Soc., Chem. Commun.* **1977**, 44–45.
142. Buffington, L. A.; Pysh, E. S.; Chakrabarti, B.; Balazs, E. A. *J. Am. Chem. Soc.* **1977**, *99*, 1730–1734.
143. Staskus, P. W.; Johnson, W. C., Jr. *Biochemistry* **1988**, *27*, 1522–1527.
144. Staskus, P. W.; Johnson, W. C., Jr. *Biochemistry* **1988**, *27*, 1528–1534.
145. Hirano, S. *Biochim. Biophys. Acta* **1973**, *329*, 152–155.
146. Hirano, S.; Kondo, S. *J. Biochem. (Tokyo)* **1973**, *74*, 861–862.
147. Hirano, S.; Kondo-Ikeda, S. *Biopolymers* **1974**, *13*, 1357–1366.
148. Gross, J. *J. Biol. Chem.* **1948**, *172*, 511–514.
149. Singley, C. T.; Solursh, M. *Histochemistry* **1980**, *65*, 93–102.
150. Hadler, N. M.; Dourmashkin, R. R.; Nermut, M. V.; Williams, L. D. *Proc. Natl. Acad. Sci. U.S.A.* **1982**, *79*, 307–309.
151. Mörgelin, M.; Paulsson, M.; Hardingham, T. E.; Heinegård, D.; Engel, J. *Biochem. J.* **1988**, *253*, 175–185.

152. Scott, J. E.; Cummings, C.; Greiling, H.; Stuhlsatz, H. W.; Gregory, J. D.; Damle, S. P. *Int. J. Biol. Macromol.* **1990**, *12*, 180–184.
153. Scott, J. E.; Cummings, C.; Brass, A.; Chen, Y. *Biochem. J.* **1991**, *274*, 699–705.
154. Scott, J. E.; Thomlinson, A. M.; Prehm, P. *Exp. Cell Res.* **2003**, *285*, 1–8.
155. Brewton, R. G.; Mayne, R. *Exp. Cell Res.* **1992**, *198*, 237–249.
156. Mikelsaar, R.-H.; Scott, J. E. *Glycoconjugate J.* **1994**, *11*, 65–71.
157. Gunning, A. P.; Morris, V. J.; Al-Assaf, S.; Phillips, G. O. *Carbohydr. Polym.* **1996**, *30*, 1–8.
158. Cowman, M. K.; Li, M.; Balazs, E. A. *Biophys. J.* **1998**, *75*, 2030–2037.
159. Jacoboni, I.; Valdrè, U.; Mori, G.; Quaglino, D., Jr.; Pasquali-Ronchetti, I. *J. Struct. Biol.* **1999**, *126*, 52–58.
160. Cowman, M. K.; Li, M.; Dyal, A.; Balazs, E. A. *Carbohydr. Polym.* **2000**, *41*, 229–235.
161. Al-Assaf, S.; Phillips, G. O.; Gunning, A. P.; Morris, V. J. *Carbohydr. Polym.* **2002**, *47*, 341–345.
162. Cowman, M. K.; Li, M.; Dyal, A.; Kanai, S. Tapping Mode Atomic Force Microscopy of Hyaluronan and Hylan A. In *Hyaluronan*; Kennedy, J. J., Phillips, G. O., Williams, P. A., Eds.; Woodhead: Cambridge, 2002; pp 109–116.
163. McIntire, T. M.; Brant, D. A. *Int. J. Biol. Macromol.* **1999**, *26*, 303–310.
164. Spagnoli, C.; Loos, K.; Ulman, A.; Cowman, M. K. *J. Am. Chem. Soc.* **2003**, *125*, 7124–7128.
165. Cowman, M. K.; Spagnoli, C.; Kudasheva, D.; Li, M.; Dyal, A.; Kanai, S.; Balazs, E. A. *Biophys. J.* **2005**, *88*, 590–602.
166. Spagnoli, C.; Korniakov, A.; Ulman, A.; Balazs, E. A.; Lyubchenko, Y. L.; Cowman, M. K. *Carbohydr. Res.* **2005**, *340*, doi:10.1016/j.carres.2005.01.024.
167. Fessler, J. H.; Fessler, L. I. *Proc. Natl. Acad. Sci. U.S.A.* **1966**, *56*, 141–147.
168. Oosawa, F. *Biopolymers* **1968**, *6*, 1633–1647.
169. Ha, B.-Y.; Liu, A. J. *Phys. Rev. Lett.* **1997**, *79*, 1289–1292.
170. Ray, J.; Manning, G. S. *Langmuir* **1994**, *10*, 2450–2461.
171. Rouzina, I.; Bloomfield, V. A. *J. Phys. Chem.* **1996**, *100*, 9977–9989.
172. Jordan, R. C.; Brant, D. A.; Cesàro, A. *Biopolymers* **1978**, *17*, 2617–2632.
173. Almond, A.; Brass, A.; Sheehan, J. K. *J. Mol. Biol.* **1998**, *284*, 1425–1437.
174. Haxaire, K.; Braccini, I.; Milas, M.; Rinaudo, M.; Perez, S. *Glycobiology* **2000**, *10*, 587–594.
175. Almond, A.; Sheehan, J. K. *Glycobiology* **2003**, *13*, 255–264.
176. Chakrabarti, B.; Balazs, E. A. *Biochem. Biophys. Res. Commun.* **1973**, *52*, 1170–1176.
177. Brisson, J.-R.; Uhrinova, S.; Woods, R. J.; van der Zwan, M.; Jarrell, H. C.; Paoletti, L. C.; Kasper, D. L.; Jennings, H. J. *Biochemistry* **1997**, *36*, 3278–3292.
178. Vercruysse, K. P.; Li, H.; Luo, Y.; Prestwich, G. D. *Biomacromolecules* **2002**, *3*, 639–643.